The bonding configuration in a partially relaxed pseudomorphic epilayer of SiGe: evidence of the BC-8 phase of silicon

2008 J. Phys.: Condens. Matter 20 335234

(http://iopscience.iop.org/0953-8984/20/33/335234)

J. Phys.: Condens. Matter **20** (2008) 335234 (7pp) doi:10.1088/0953-8984/20/33/335234

The bonding configuration in a partially relaxed pseudomorphic epilayer of SiGe: evidence of the BC-8 phase of silicon

M Pandey[1,4], S K Ray[2] and P Selvam[3]

[1] High Pressure Physics Division, Bhabha Atomic Research Centre, Mumbai-400085, India
[2] Department of Physics and Meteorology, Indian Institute of Technology, Kharagpur-721302, India
[3] Department of Chemistry, Indian Institute of Technology-Madras, Chennai, India

E-mail: mpandey@barc.gov.in and m.pandey@fzd.de

Received 18 April 2008, in final form 16 June 2008
Published 31 July 2008
Online at stacks.iop.org/JPhysCM/20/335234

Abstract

The bonding configuration of a silicon host lattice in a carbon-induced partially relaxed pseudomorphic epilayer of SiGe is studied using x-ray photoelectron spectroscopy, high-resolution XRD and Raman spectroscopic techniques. In-plane and out-of-plane strains are estimated using high-resolution x-ray diffraction. Careful analysis of the x-ray photoelectron spectra (XPS) suggests that the bonding environment of the silicon host lattice is modified, and is attributed to the presence of graphite-like-sp^2 bonding in addition to the tetrahedral-sp^3 bonding. These results are further supported by our Raman studies. Our Raman studies indicate the presence of the BC-8 phase; a high-pressure phase of silicon. The modified configuration of the silicon host lattice at high pressure is responsible for the observed changes in the XPS and Raman spectra. These results are also compared with the carbon incorporated silicon epilayers ($Si_{1-x}C_x$) having negligible strain relaxation. We attribute these effects to the strain-induced effects and not to the compositional effects of Ge.

(Some figures in this article are in colour only in the electronic version)

1. Introduction

Strained epilayers of SiGe find applications in silicon technology, including hetero-junction bipolar transistors (HBTs) and hetero-junction MOSFETs [1–3]. The extremely high carrier mobility in this system at low temperature makes it useful in high-speed electronic applications [4]. Its usage as thermoelectric devices is also promising [5]. It is well known that incorporating germanium in silicon introduces a compressive strain and therefore has a limitation on the critical thickness of the strained layer up to which the epitaxy can be maintained. Incorporating smaller sized carbon atoms in the strained layer of a SiGe system, relaxes part of the strain allowing thicker films to grow pseudomorphically. Recently, Jang *et al* [6] studied the effect of strain relaxation by annealing the strained layers at higher temperatures and Mamor *et al* [7] studied the effect of strain relaxation by He ion irradiation on the band gap. They observed that the relaxation of strain results in the generation of a variety of defects (especially the misfit and the threading dislocations) deteriorating their crystalline quality, and in turn affecting the device performance. In our studies, we introduced partial relaxation of the strain by incorporating ∼1% carbon during the growth process in the $Si_{0.7}Ge_{0.3}$ strained epilayer. According to Mamor *et al* [7], the effect of Ge composition (other than the strain effects) is equally important while dealing with systems when the strain is relaxed by incorporating smaller sized atoms, such as carbon in our case. Thus, in order to differentiate between the compositional effects from the strain-induced effects, we also studied the strained epitaxial layer of $Si_{1-x}C_x$ ($x = 0.62\%$). This value of carbon incorporation ensured negligible strain relaxation in $Si_{1-x}C_x$ epitaxial layers, and has therefore served the important purpose of isolating the effects of Ge

[4] Author to whom any correspondence should be addressed. On leave from the Institute of Ion Beam Physics and Materials Research, Forschungszentrum Dresden-Rossendorf, Dresden D-01314, Germany.

composition from that of the strain-induced effects. It may be noted that strain relaxation by carbon incorporation is widely used for band gap variation in these materials, and therefore this study is quite important from the point of view of basic understanding.

Our interest in the present study is also motivated towards investigating effects of high-pressure conditions on the host silicon lattice. The magnitude of strain present in the sample under study will result in built-in high-pressure conditions. At such high pressures silicon undergoes changes in the bonding, leading to changes in its electronic as well as phonon band structure. Polymorphism in silicon and germanium under extreme high-pressure conditions has already been studied by various researchers [8–11]. Evidence of high-pressure phases in silicon during nano-grinding has been reported by Ruffell *et al* [12] and during nano-indentation in silicon by Wang *et al* [13]. Since a similar situation is present in our samples as well this study will help us to investigate changes in the bonding configuration of the silicon host lattice.

We employed high-resolution XRD studies to understand the nature of strain present in the samples i.e. whether the sample is experiencing a compressive strain or a tensile strain. In addition, it has been used to estimate the in-plane and out-of-plane strain components present in the samples. X-ray photoelectron spectroscopy (XPS) is used to investigate the bonding configuration of the silicon host lattice. Raman studies clearly indicate the presence of a high-pressure phase. Our studies have suggested a structural modification in the silicon host lattice, and have further suggested that this modification is due to the presence of a high-pressure phase in the samples.

2. Experimental details

Carbon incorporated epitaxial layers of Si–Ge and Si systems, i.e. a compressively strained $Si_{0.69}Ge_{0.3}C_{0.01}$ (sample S1) and a tensile strained $Si_{0.994}C_{0.006}$ (sample S2) on silicon substrates were respectively grown using ultrahigh vacuum chemical vapour deposition (UHV-CVD) and molecular beam epitaxy (MBE), respectively. An epitaxial layer of $Si_{0.69}Ge_{0.3}C_{0.01}$ having a thickness of ∼30 nm was grown at 550 °C using SiH_4 and GeH_4. An epitaxial layer of pseudomorphic alloy with composition $Si_{0.994}C_{0.006}$ having a thickness of ∼100 nm was grown using solid source MBE at a temperature of 500 °C. This was the value of carbon, which could be safely incorporated in silicon with negligible strain relaxation. The details of the sample growth are reported elsewhere [14].

Strain analysis was carried out on a Philips (X'Pert MRD) high-resolution XRD (HRXRD) using monochromatic Cu Kα_1 radiation (λ = 1.540 5980 Å) in a range of ∼2° about the Bragg peak at an interval of 0.001°. The chemical composition of these films was studied using x-ray photoelectron spectroscopy (XPS) with Mg Kα (energy = 1253.6 eV) radiation on a thermo-8017 spectrometer. The instrumental resolution together with the width of Mg Kα radiation was ∼0.8 eV. A careful analysis of Si 2p and C 1s spectra was used to study the bonding configuration on these samples. Since, XPS is sensitive to the surface layers (i.e. few nano-meters), the samples were sputtered (inside the vacuum chamber) for 5 min before recording the XPS spectra to remove the top contaminated layer. In semiconducting samples, the emission of the photoelectrons results in the polarization of surrounding electrons that screens the suddenly created hole during the photoemission process. This moves the Fermi level of the spectrometer by as much as its bandgap. In order to avoid this problem, we coated the samples with an ultrathin layer of Sn. Even with Sn coating, some charging effects were observed, which were corrected using C 1s peak as a reference. Raman spectra were recorded on a JOBIN-YOBIN HR-800 spectrometer using an excitation wavelength of ∼5145 Å with a resolution of ∼1 cm^{-1}.

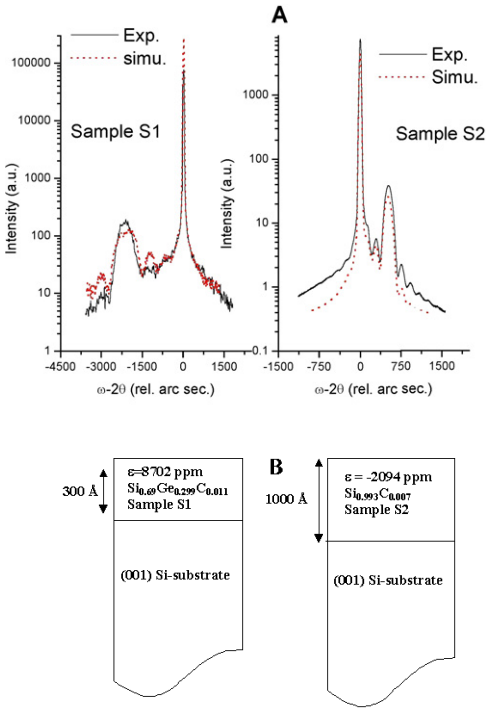

Figure 1. (A) High resolution (exp. and simu.) of sample S1 (left) and sample S2 (right) of (004) symmetric reflection XRD plots. (B) The layer structure of both samples along with the thickness and the in-plane strain.

3. Results and discussions

High-resolution XRD of the (004) orientation of silicon shows a layer peak in addition to the substrate peak at lower and higher angle (with respect to the substrate peak) respectively for samples S1 and S2 (figure 1(A)). This indicates that the sample S1 is under compressive strain and the sample S2 is under tensile strain. In order to estimate the in-plane and out-of-plane strains, one needs to record the asymmetric reflections as well. The corresponding asymmetric reflections ((113) and (331) in the case of S1 and (113) and (224) in case of S2) are shown in figure 2. The substrate peak, layer peak and buffer layer peaks (marked with S, L and B, respectively) are clearly visible in these asymmetric reflections. Rocking curves along (004) of S1 and S2 are simulated taking into consideration the composition, thickness and their respective lattice mismatch. Here the lattice mismatch (Δ) is given

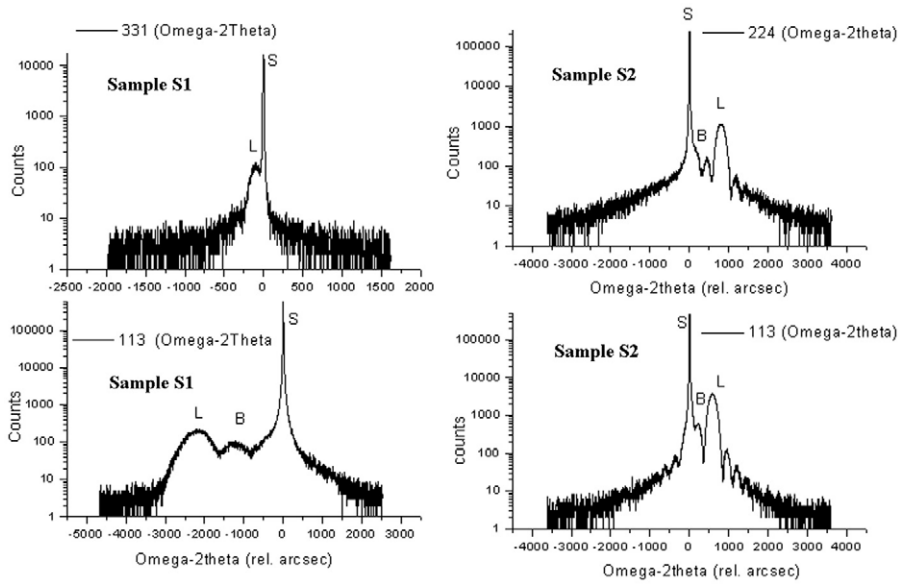

Figure 2. Rocking curves for asymmetric reflections for samples S1 (left) and S2 (right). The substrate, layer and the buffer layer are marked with S, L and B, respectively.

by: $\Delta = (a_{\text{layer}} - a_{\text{substrate}})/a_{\text{substrate}}$, where a_{layer} is the lattice parameter of the layer with respect to the Si substrate. The simulations are carried out using the kinematic intensity simulations, as described by Picraux *et al* [15]. This includes appropriate values of atomic structure factor for Si, Ge and C (diamond) at $\lambda = 1.5406$ Å, and their corresponding elastic constants [16]. Estimation of strain relaxation is also carried out using these simulations. For a perfect epitaxial layer, the relaxation is nearly zero, whereas departure from epitaxial nature is introduced via the relaxation. The simulations for sample S1 yields a composition: $Si_{0.69}Ge_{0.299}C_{0.011}$, thickness ∼300 Å and a relaxation of 40%, while for sample S2 yield composition: $Si_{0.993}C_{0.0061}$, thickness ∼1000 Å and almost negligible relaxation (<5%). In-plane and out-of-plane strains in both cases have been estimated using the tetragonal distortion model [15]. Accordingly, the peak position relative to the substrate $\Delta\omega_{\text{LS}}$ is related to the change in (hkl) plane spacing Δd and the rotation of the planes $\Delta\psi$ given by:

$$\Delta\omega_{\text{LS}} = (\Delta d/d_{hkl}) \tan\theta_{\text{B}} + \Delta\psi, \qquad (1)$$

where $\Delta d/d_{hkl} = \varepsilon_{\perp} \cos^2\psi + \varepsilon_{\parallel} \sin^2\psi$ and $\Delta\psi = \pm(\varepsilon_{\perp} - \varepsilon_{\parallel}) \sin\psi \cos\psi$. The plus (+) or minus (−) sign is selected depending upon whether ω_0 is equal to $\theta_{\text{B}} - \psi$ or $\theta_{\text{B}} + \psi$ i.e. grazing incidence or grazing exit. θ_{B} is the Bragg angle corresponding to the substrate and ψ is the angle which the diffracting plane makes with the surface of the substrate. $\varepsilon_{\perp}$ and $\varepsilon_{\parallel}$ are the out-of-plane and in-plane strains, which are measured relative to the substrate, and are estimated from the rocking curves of different symmetric and asymmetric planes (as given in figures 1 and 2). It must be mentioned that while $\varepsilon_{\perp}$ can be estimated simply by recording a symmetric plane, $\varepsilon_{\parallel}$ requires the recording of both symmetric and asymmetric planes [17]. We have estimated $\varepsilon_{\perp}$ and $\varepsilon_{\parallel}$ using equation (1). These values for sample S1 are estimated to be 12.812×10^{-3} and -0.236×10^{-3}, respectively. Corresponding values for sample S2 are -3.441×10^{-3} and -0.124×10^{-3}, respectively. The (331) reflection in sample S2 is merged with the substrate (the two being quite close). We have estimated that 1% carbon incorporation is able to relax ∼40% strain in sample S1. This relaxation in sample S2 is found to be negligible. The structure of the samples S1 and S2 in terms of thickness and the in-plane strain are given in figure 1(B). It may be noted that the low value of $\varepsilon_{\parallel}$ in sample S2 indicates that the in-plane lattice parameter is quite close to that of crystalline silicon, indicating its pseudomorphic nature. The layer to substrate peak separation ($\Delta\omega_{\text{LS}}$), % of strain relaxation and the estimations of $\varepsilon_{\parallel}$ and $\varepsilon_{\perp}$ are given in table 1.

Table 1. Details of asymmetric reflections used in estimating in-plane strain ($\varepsilon_{\parallel}$) and out-of-plane strain ($\varepsilon_{\perp}$).

	Sample S1		Sample S2	
hkl	113	331	113	224
$\Delta\omega_{\text{LS}}$ (radians)	1.07×10^{-2}	1.95×10^{-2}	2.67×10^{-3}	3.88×10^{-3}
$\varepsilon_{\parallel}$	-0.236×10^{-3}		-0.124×10^{-3}	
$\varepsilon_{\perp}$	12.812×10^{-3}		-3.441×10^{-3}	
% strain relaxation	40%		<5%	

The detailed analysis of the XPS spectra on the cleaned surfaces has been carried out after applying a peak fitting procedure to the Si 2p, C 1s and Ge 3d spectra and is shown in figures 3(A), (B) and (D), respectively. The Si 2p and C 1s spectra of samples S1 and S2 can be compared with that of pure silicon substrate and graphite (figure 3(C)). It may be noted that the asymmetry of the Si 2p line observed in the XPS spectra of pure crystalline silicon used as a reference sample (as shown in figure 3(C)), is mainly due to the spin–orbit interaction and the different weights attached to the 1/2 and 3/2 components [18]. The asymmetry of this peak as obtained by half width at half

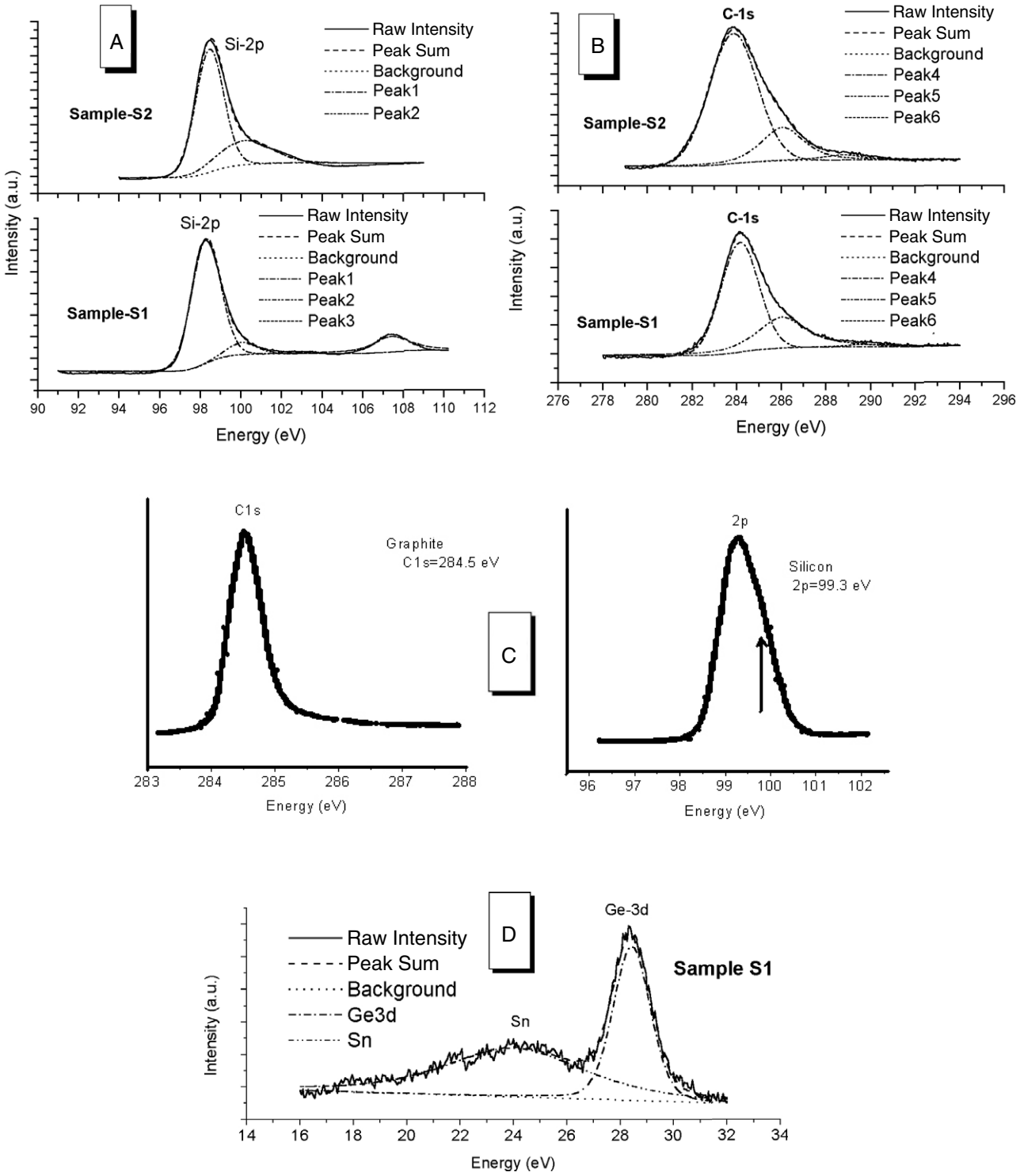

Figure 3. XPS spectra of Si 2p (A) and C 1s (B) for samples S1 and S2 after removing the top contaminated layer. Si 2p and C 1s spectra of pure silicon and graphite for comparison with the sp^3 bonded silicon and sp^2 bonded carbon. (C) The asymmetry in the Si 2p spectra is marked with an arrow. Also shown is the Ge 3d spectrum for sample S1 (D).

maxima on the left ($FWHM_{left}$)/half width at half maxima on the right ($FWHM_{right}$) is ∼1.35 and the full width at half maxima of this peak is found to be ∼1.4 eV.

The C 1s, Si 2p and Ge 3d spectra are fitted with a sum of more than one peak. The fitting procedure involves the position, width and intensity of individual peaks. It must be mentioned that the G/L ratio in all spectra is chosen to be a free fitting parameter, and we have found that the Gaussian contribution is more than 95% in all cases. Also the width and the asymmetry of the Si 2p (responsible for the spin–orbit splitting) as observed for the crystalline silicon is taken into consideration. We have assumed a Shirley background [19]

Table 2. Details of fitting parameters for C 1s, Si 2p and Ge 3d peaks of x-ray photoelectron spectroscopy after removing the top contaminated layer.

Peak	Sample1			Sample2		
	Position (eV)	Width (eV)	Relative intensity	Position (eV)	Width (eV)	Relative intensity
Si 2p	98.27 (Pk1)	1.68	1.00	98.45	1.64	1.00
	100.04 (Pk2)	1.71	0.10	100.19	3.08	0.37
	107.40 (Pk3)	2.19	0.22	—	—	—
C 1s	283.84 (Pk4)	2.54	1.00	284.14	1.99	1.00
	286.06 (Pk5)	2.21	0.28	286.02	2.53	0.49
	288.77	2.078	0.05	289.64	1.98	0.03
Ge 3d	24.02	6.22	0.73	—	—	—
	28.43	1.65	1.00	—	—	—

to be present in all these spectra. The details of the fitting parameters in terms of position, width and the relative intensity for Si 2p, C 1s and Ge 3d are given in table 2. The peak intensity is normalized with respect to the most intense peak in both cases. In addition to a peak at ∼98.0 eV (Pk1), we also observe a peak at ∼100 eV (Pk2) in both samples. The relative intensity of peak-Pk2 in sample S2 is approximately three times higher than that observed in sample S1. An additional peak (Pk3) at 107 eV due to the Ge LMM Auger transitions is also observed in sample S1. C 1s spectra of these samples show peaks at ∼284 eV (Pk4) and at 286 eV (Pk5). The relative intensity of the latter peak i.e. Pk5 is more in the case of sample S2 (∼2 times). Finally, a very low intensity peak (Pk6) having intensity ∼3–5% of the main peak is also present, which is attributed to a slight contamination due to the adsorbed C–O molecules. A peak at ∼28 eV in the Ge 3d spectra is also observed in sample S1, which is absent for sample S2. An additional peak at ∼24 eV in the Ge 3d spectra related to the ultrathin layer of Sn (intentionally coated on both the samples) is also seen.

According to previous studies, polymorphism in elemental silicon is observed under high-pressure conditions [9]. Under the present conditions of biaxial strain a similar situation appears to prevail in both the samples. When the diamond phase (FC-2) of silicon under compression is partially relaxed, one obtains the body centred cubic phase (BC-8 form). The confirmation of this phase in our samples comes from the Raman spectra as shown in figure 4. A peak at ∼432 cm^{-1} typical of the BC-8 form of silicon [8, 13], is invariably present in both the samples. Similar peaks have been observed by Eberl *et al* [20] and Finkman *et al* [21] in partially relaxed pseudomorphic layers. Peaks corresponding to other vibrations, say, the epilayer peak at ∼508 cm^{-1} (in sample S1), ∼Si–Ge peak at 407 cm^{-1} (in sample S1) and C local modes at ∼615 cm^{-1}, 670 cm^{-1} and 820 cm^{-1} (in both the samples) are also marked in this figure. The fully relaxed layer for 30% Ge component will exhibit a Raman peak at ∼500 cm^{-1}. This difference in the observed Raman peak and the calculated one for the fully relaxed alloy, which in our case is ∼10 cm^{-1}, is a measure of the internal stress present in the sample. This difference in the value of the Raman shift indicates a biaxial stress of ∼2 GPa in sample S1 as calculated from the calibration curve given by Dietrich *et al* [22].

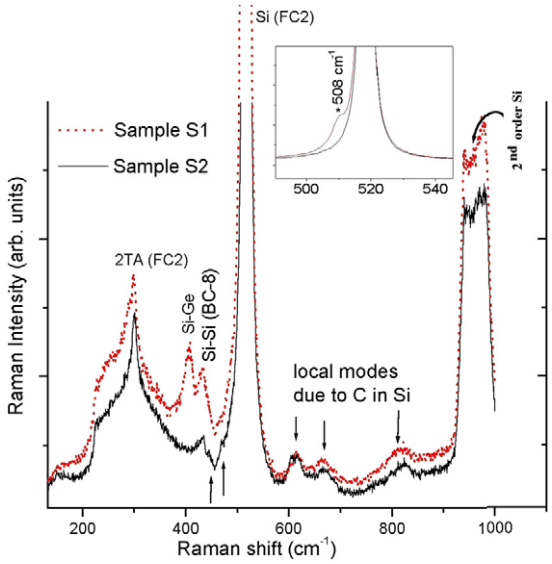

Figure 4. Raman spectra of sample S1 and S2, indicating peaks due to BC-8 and FC2 forms of silicon. Peaks due to Si–Ge and the local modes of carbon (marked by arrows) are also indicated.

We further notice, from the presence of local carbon modes, that carbon in silicon host lattice exists in different configurations. The tetrahedral (T_d) arrangement of silicon has the T_2 symmetry of vibration. When one of the Si atom is substituted by a C atom, the symmetry is lowered to C_{3v} and the T_2 mode of vibrations is split into the A and E modes of vibration. As reported by Hoffmann *et al* [23], the Raman peak at ∼615 cm^{-1} is related to the A mode of vibrations, while the E mode is observed at 670 cm^{-1}. The strained epilayers with very low carbon content show only the first peak (∼615 cm^{-1}) [21]. The latter peaks (∼670 and 820 cm^{-1}) are seen only in samples having a significant amount of carbon content [24]. It has been observed by Finkman *et al* [21] that the shoulder peak at ∼615 cm^{-1} develops into a well-defined peak with a significant blue shift when the carbon concentration in the SiGe epilayer is increased.

The self-consistent charge density-functional-based tight binding method employed by Zhu *et al* [25], indicates that the carbon incorporation in silicon can generate a variety of geometrical re-arrangements. One of the situations is that carbon occupying the substitutional sites C_{sub} (figure 5(A)), where the total energy minimization yields a configuration in which the Si–C bond is longer (∼2.03 Å) than the normal SiC (1.91 Å). The bond angle between the C_{sub} and the adjacent silicon neighbours is 110°, close to that of the tetrahedral sp^3 bonded silicon (109.5°) [25]. Thus the Raman peak at ∼615 cm^{-1} is related to carbon occupying these C_{sub} sites, as at low concentration most of the carbon goes into substitutional positions. The carbon atom can however also exist at an interstitial position (C_{int}), located midway between the Si atoms of the two tetrahedra (figure 5(B)) [25]. This will result in asymmetric Si–C bonds (namely 1.76 and 1.83 Å) and Si–Si back bonds (having bond lengths of ∼2.29 and 2.46 Å quite different from that of an ideal one). The bond angle around this mid-bond carbon atom, can be as large as 124° favouring an sp^2

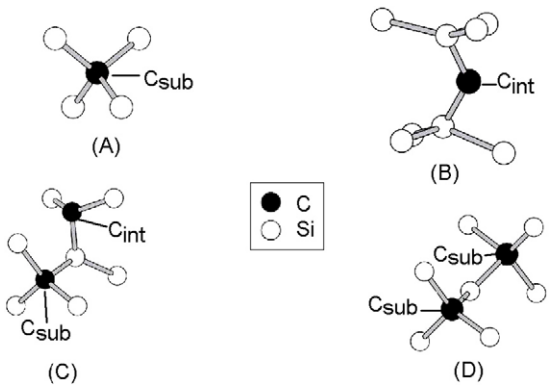

Figure 5. Different configurations in which carbon can exist in silicon host lattice: (A) substitutional C_{sub}, (B) interstitial C_{int}, (C) substitutional–interstitial (C_{sub}–C_{int}) and (D) substitutional–substitutional (C_{sub}–C_{sub}).

kind of re-hybridization [25]. The Raman peak at ∼670 cm^{-1} may be associated with this kind of configuration. The Raman peak at ∼810 cm^{-1} might have its origin in a bi-carbon complex like C_{sub}–C_{int} and C_{sub}–C_{sub} (as shown in figures 5(C) and (D)). The theoretical phonon spectral density calculated for these complexes is reported to have peaks at ∼485 and 810 cm^{-1} [25]. The peak at ∼810 cm^{-1} is clearly seen in the respective Raman spectra of samples S1 and S2. The 485 cm^{-1} peak seems to have merged into the Raman signal of BC-8 silicon (∼432 cm^{-1}) and the layer peak at ∼508 cm^{-1}, and therefore does not appear in the Raman spectra.

Coming to the high-pressure phase of silicon, the BC-8 form as reported by Pfrommer *et al* [10], using density functional theory under local density approximation, can be imagined as if the lattice comprising of silicon atoms is arranged in an irregular hexagonal array of the twisted-boat form. Each Si atom is connected to three longer bonds (A ∼ 2.39 Å) and a shorter bond (B ∼ 2.31 Å). The corresponding bond length for the FC-2 phase is ∼2.35 Å. The bond angles in the BC-8 phase are found to be 118° and 99° i.e. significantly different from that of a regular tetrahedral FC-2 form having bond angles ∼109.5°. The Si atom with a shorter bond length will show higher binding energy. Thus, the two-peak nature of Si 2p spectra (i.e. Pk1 and Pk2 as mentioned above) can be attributed to the BC-8 phase of silicon. Their intensity ratios also follow the longer to shorter bond distributions (i.e. 3:1 ratio). A theoretical study carried out by Cabrera *et al* [26] suggested that for Si–Si the bond length is shorter than 2.21Å, graphite like sp^2-bonding in silicon is favoured. Although, the bond length 'A' in BC-8 is slightly more than that suggested by Cabrera *et al* [26], a tendency towards sp^2 configuration of silicon cannot be ruled out. Further confirmation of sp^2 bonding is indicated in the C 1s spectra, where we have observed an intense peak at ∼284 eV and a shoulder peak at ∼286 eV. It needs to be mentioned that the sp^2 and sp^3 bonded carbon shows peaks at 284 and 286 eV, respectively [27]. Thus, the presence of additional peaks in the C 1s and Si 2p spectra, suggests the presence of at least two different configurations of host silicon atoms. Since similar peaks are obtained in both samples S1 and S2, we can presume that they are related to the strain in the samples and not the Ge related compositional effects. The presence of a Raman peak at ∼432 cm^{-1} (corresponding to the high-pressure phase) in both the samples further corroborates these arguments. We would also like to mention that these results are of great consequence towards explaining the strain-induced variation in defect centres and the band gap variation recently reported by Mamor *et al* [7]. Our result also provides the microscopic origin of the phonon spectrum of relaxed $Si_{1-x}Ge_x$ alloys [28].

The phase transformation due to the bond shortening effects i.e. transformation from regular FC-2 to BC-8 is very easy to understand. The incorporated Ge has the effect of expanding the lattice parameter via increases in the cell volume. Here, the epitaxial nature of the sample tends to maintain the a–b parameter close to that of crystalline silicon, forcing the 'c' parameter to reduce. This will lead to an anisotropic stress in sample S2, and will thereby modify the bonding configuration of the host silicon lattice. Thus, the anisotropy in stress introduced will result in a modified tetrahedral configuration of silicon. With some of the bonds being shorter and some being longer, distortion in the tetrahedral geometry of the silicon network is bound to happen. This is further supported by the work of Woicik *et al* [29], where extensive EXAFS studies have suggested bond angle distortions in highly strained Si–Ge epilayers. In sample S2, i.e. tensile strained $Si_{1-x}C$, the carbon incorporation in the silicon lattice results in the reduction of the lattice volume and hence in the Si–Si bond length. The epitaxial nature of the sample, however, tends to maintain the in-plane lattice parameter i.e. the a–b parameter is increased from its equilibrium value. Since the volume has to be constant, the 'c' parameter is shortened. Thus, in both cases, a situation similar to the graphite like sp^2 configuration is favoured, which in turn results in the BC-8 phase. We believe that the presence of a high-pressure phase will also explain some of the unexplained facts, in particular the observed Raman shifts as a function of strain relaxation, and might suggest an alternate approach towards understanding the microstructure of these samples.

4. Conclusions

We have studied the carbon-induced partially strain compensated $Si_{0.69}Ge_{0.3}C_{0.01}$ and tensile strained $Si_{0.994}C_{0.006}$ alloys under biaxial strain. High-resolution XRD of a previous sample shows a layer peak at the left, whereas in the later sample it shows a peak at the right of the intense substrate peak, indicating respectively the compressive and tensile strain. High-resolution XRD studies have further been utilized to simulate the layer structure and to estimate the in-plane and out-of-plane strain in these samples, indicating the presence of bi-axial strain. XPS studies in these samples suggest two different bonding configurations of the silicon lattice. In addition to the normal sp^3 configuration, graphite like sp^2 bonding is also favoured for short Si–Si bond lengths. This is further supported by the C 1s spectrum as an additional peak observed at a higher value of binding energies. The Raman studies clearly show

formation of the BC-8 phase of silicon in both the samples, indicating that it is not the compositional effects but the strain-induced effects responsible for the change in bonding configuration. Our investigations may find an alternate approach towards understanding the microstructure in these samples.

Acknowledgments

The authors are grateful to Professor S K Banerjee of the University of Texas at Austin for the growth of the SiGeC sample. One of the authors (MP) is also grateful to Dr T Sakuntala and Dr S M Sharma for their constant support in carrying out this work. Our special thanks also go to the Department of Information Technology, Government of India for providing support in the form of a sponsored research project. We also thank Dr D S Misra, Physics Department, IIT-Bombay and the Central Surface Analytical Facility, IIT-Bombay for help in using their Raman and XPS facilities.

References

[1] Kasper E and Paul D J 2005 *Silicon Quantum Integrated Circuits: Silicon–Germanium Hetrostructure Devices—Basics and Realization* (Berlin: Springer)
Cressler J D 2006 *Silicon Hetrostructure Hand Book: Materials, Fabrication and Applications of SiGe and Si Strained Layer Epitaxy* (New York: Tayler and Francis)
[2] Jain S C and Hayes W 1991 *Semicond. Sci. Technol.* **6** 547
[3] Paul D J 2004 *Semicond. Sci. Technol.* **19** R75–108
[4] Fortuna V A, Dollfus P and Retailleau S G 2005 *Solid State Electron.* **49** 1320
Kar G S, Dhar A and Ray S K 2000 *J. Appl. Phys.* **88** 2039
[5] Wagner M, Span G and Grasser T 2006 *Int. Si–Ge Technology and Device Mtg—2006 (IEEE)* p 216 (Cat. No. 06EX1419)
Druzhinin A A, Ostrovskii I P and Kognt I R 2006 *Int. Si–Ge Technology and Device Mtg—2006 (IEEE)* p 78 (Cat. No. 06EX1419)
[6] Jang J H, Phen M S, Gerger A, Jones K S, Hansen J L, Larsen A N and Cracium V 2008 *Semicond. Sci. Technol.* **23** 35012
[7] Mamor M, Elzain M, Bouziane K and Harthi S H 2008 *Phys. Rev.* B **77** 35213
[8] Goldberg A, Batanoung M E and Wooten F 1982 *Phys. Rev.* B **26** 6661
[9] Crain J, Clark S J, Ackland G J, Payne M C, Milman V, Hatton P D and Reid B J 1994 *Phys. Rev.* B **49** 5329
[10] Pfrommer B G, Cote M, Louie S G and Cohen M L 1997 *Phys. Rev.* B **56** 6662
[11] Nelmes R J, McMahon M I, Wright N G and Allan D R 1993 *Phys. Rev.* B **48** 9883
[12] Ruffell S, Bradby J E and Williams J S 2006 *Appl. Phys. Lett.* **89** 91919
[13] Wang Y, Zou J, Huang H, Zhou L, Wang B L and Wu Y Q 2007 *Nanotechnology* **18** 465705
[14] John S, Quinones E J, Farguson B F, Ray S K, Mullins C B and Banerjee S K 1996 *Mater. Res. Soc. Symp. Proc.* **440** 275
[15] Picraux S T, Douyle B L and Tsao J Y 1992 *Semiconductors and Semimetals* vol 33, ed T P Pearsall (New York: Academic) p 139
[16] Brown P J *et al* 1999 *International Tables for Crystallography* 2nd edn, vol c, ed A J C Wilson and E Prince (Norwell: Kluwer–Academic)
[17] Nair G P, Chandrasekaran K S, Narsale A M, Arora B M and Gokhale M R 2001 *Nucl. Instrum. Methods* B **184** 515
[18] Thomas T D, Miron C, Wiesner K, Morin P, Carroll T X and Saethre L J 2002 *Phys. Rev. Lett.* **89** 223001
[19] Castle J E and Salvi A M 2001 *J. Vac. Sci. Technol.* A **19** 1170
[20] Eberl K, Iyer S S, Zollner S, Tsang J C and LeGoues F K 1992 *Appl. Phys. Lett.* **60** 3033
[21] Finkman E, Meyer F and Mamor M 2001 *J. Appl. Phys.* **89** 2580
[22] Dietrich B, Bugial E, Klatt J, Lippert G, Morgenstern T, Osten H J and Zaumseil P 1993 *J. Appl. Phys.* **74** 3177
[23] Hoffmann L, Nielsen B B, Larsen A N, Leary P, Jones R, Briddon P R and Oberg S 1999 *Phys. Rev.* B **60** 13573
[24] Dashiell M W, Kulik L V, Hits D and Kolodzey J 1998 *Appl. Phys. Lett.* **72** 833
[25] Zhu U Y, Lee S M, Kim J Y, Lee Y, Chung D C and Frauenheim T 2001 *Semicond. Sci. Technol.* **16** R41
[26] Cabrera M F, Munoz A, Windl W, Demkov A A and Sankey O F 1999 *Modelling Simul. Mater. Sci. Eng.* **7** 929
[27] Diaz J, Paolicelli G, Ferrer S and Comin F 1996 *Phys. Rev.* B **54** 8064
[28] Pezzoli F, Sanguinetti S, Bonera E, Grilli E and Guzzi M 2007 *J. Phys. Conf. Ser.* **92** 12152
[29] Woicik J C, Bouldin C E, Bell M I, Cross J D, Tweet D J, Swanson B D, Zhang T W, Sorensen L B, King C A, Hoyt J L, Pianetta P and Gibbons J F 1991 *Phys. Rev.* B **43** 2419